Linear Array Deformable Mirror

with Fast and Precise Laser Pulse Compression Application Overview and Pulse Compression for Two-Photon Microscopy Application Demonstration

Prototype Device Overview

The Linear Array 1x140 actuator Deformable Mirror (DM), shown in Figure 1, was developed for use in laser pulse shaping applications in which the DM is used to modify the phase of the spectral components of the laser pulse to achieve a desired temporal pulse characteristic. The device design is a based on BMC's heritage deformable mirror technology that uses hysteresis-free electrostatic actuators to deform a continuous or segmented mirror facesheet.

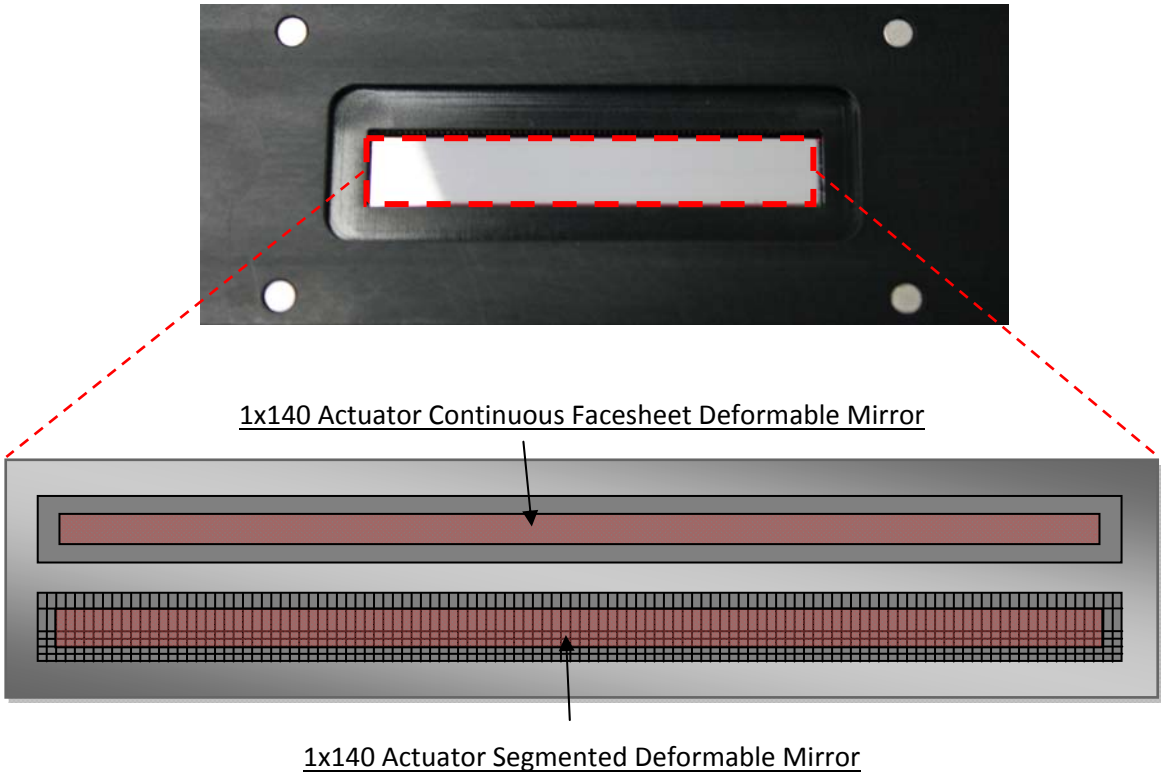

Figure 1. Image of an aluminum coated BMC Linear Array 1x140 actuator DM. This prototype device has both a segmented and continuous facesheet DM that lie parallel to each other on the same die for performance evaluation and comparison.

As illustrated in Figure 2, the device structure consists of actuator electrodes underneath a double cantilever flexure that is electrically isolated from the electrodes and maintained at a ground potential. The actuators are arranged in a 1x140 grid, on a pitch of 300µm, and the

flexible mirror surface is connected to the center of each actuator through a small attachment post that translates the actuator motion to a mirror surface deformation.

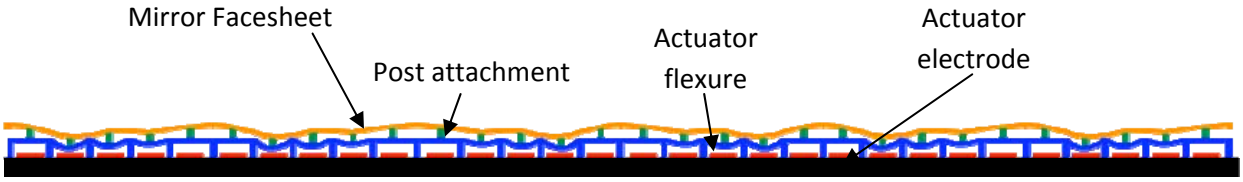

Figure 2. Cross sectional schematic of an electrostatic MEMS DM. A compliant mirror facesheet is attached to an array of posts (green), each centered on an electrostatic actuator comprised of a flexible cantilever (blue) suspended over a fixed electrode (red), all fabricated using semiconductor fabrication processes on a silicon wafer (black).

To deform the mirror facesheet a voltage is applied to the actuator electrode which attracts the grounded cantilever flexure, thereby locally deforming the post and the mirror. This MEMS DM architecture allows for local deformation of the mirror membrane with an influence function of 0% and 20% on its nearest neighbor for a segmented and continuous facesheet DM, respectively (see Figure 3). This allows the DM to take on high order shapes to modify an incident wavefront.

Continuous Facesheet DM **Segmented Facesheet DM**

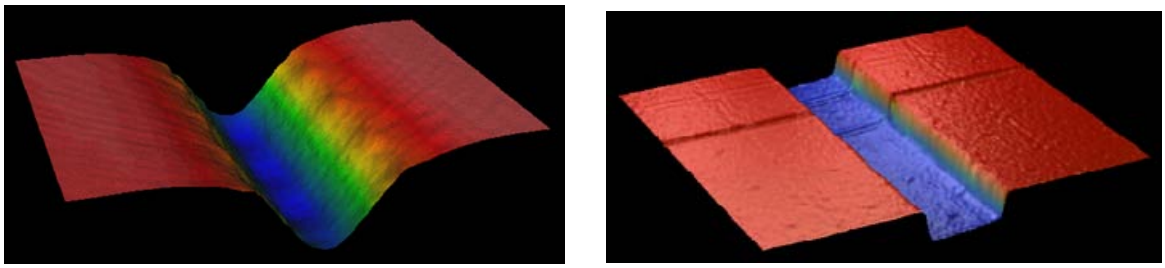

Figure 3. Surface measurements of a 1x5 sub-aperture of a continuous (Left) and segmented (Right) facesheet DM with a single actuator deflected showing the local influence on its neighboring actuators - ~20% of maximum stroke for the continuous facesheet device; 0% for a segmented DM.

Electrostatics is used to achieve mirror deformation at each actuation point using an actuator, as illustrated in Figure 4. The actuator has an initial gap, ***g***, between the flexure and the fixed electrode. An applied potential, ***V***, results in an attractive electrostatic force that bends the actuator membrane downward. As the flexure bends, an elastic (mechanical) restoring force acts in the opposite direction. At equilibrium these two forces balance and the equilibrium deflection at the membrane mid-span is ***z***. The equilibrium deflection is a nonlinear increasing function of ***V***. The equilibrium is stable until the voltage is raised to a point where the equilibrium deflection is equal to approximately ½ of the initial gap. Above that voltage, electrostatic forces are so large that they cannot be balanced by mechanical restoring forces, and the actuator membrane crashes unstably into the fixed electrode. In practice, this unstable region is generally avoided.

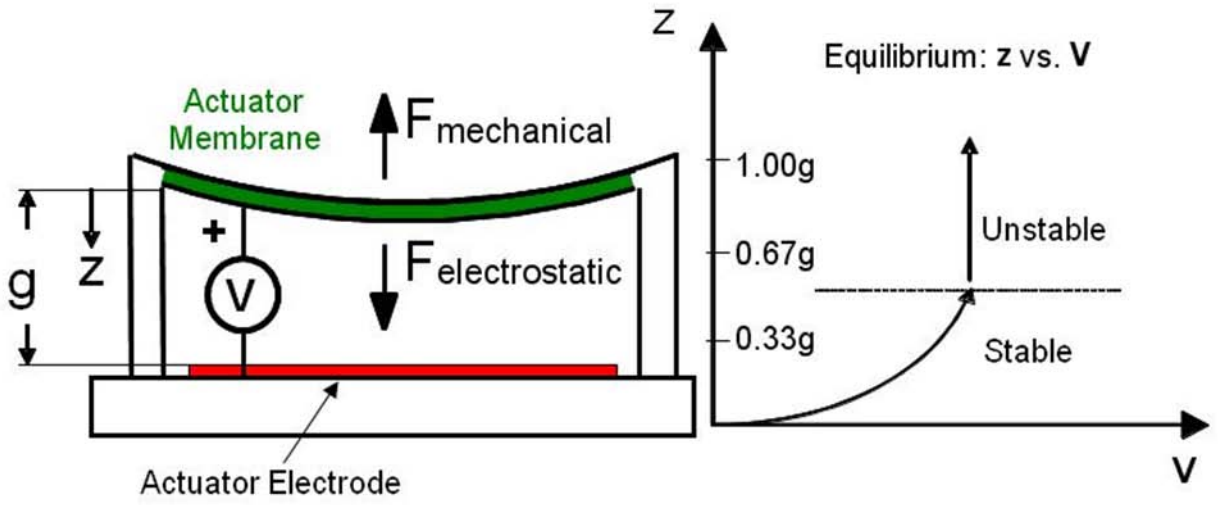

Figure 4. Schematic of electrostatic actuation of a double cantilever actuator used in the MEMS deformable mirror design. The MEMS DM consists of a 1-D array of these actuators each supporting a post attached to the back of the flexible mirror facesheet (not shown in illustration).

Each actuator can be controlled independently to drive the DM surface to the desired shape. Figure 5 shows some example low and high order shapes on a 1x32 sub-aperture of the continuous facesheet DM. These shapes were achieved by applying pre-defined voltages to each of the DM actuators resulting in the desired surface deformation.

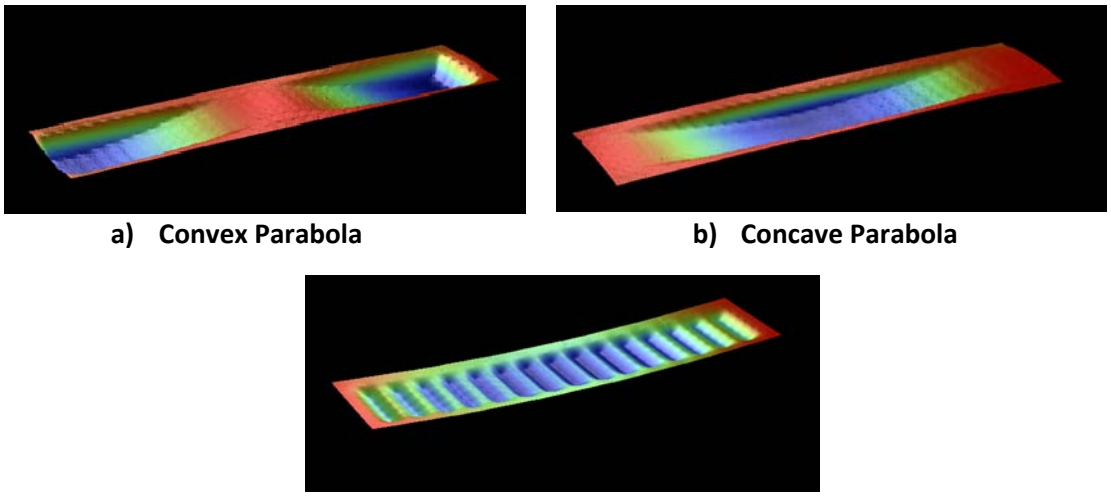

a) Convex Parabola **b) Concave Parabola**

c) Ripple

Figure 5. Surface measurements of example shapes applied to a 1x32 sub-aperture of a continuous facesheet DM. Pre-defined voltage maps applied to the device using 14-bit resolution DM drive electronics result in a convex (a) and concave (b) parabolic shape with a 2µm amplitude, and a high order ripple shape (c).

Continuous and Segmented DM Configuration

The prototype deformable mirror device has both a continuous and segmented mirror facesheet version as shown in Figure 6 below, with an active area of 1.2mm x 41.7mm and 1.5mm x 42mm respectively. The active mirror area is supported by an array of 5x140 electrostatic actuators, spaced at a pitch of 300µm, in which each row of five actuators are ganged together and act in concert. The active DM area is surrounded by two rows of dummy (inactive) actuators required to optimize device optical quality and electromechanical performance.

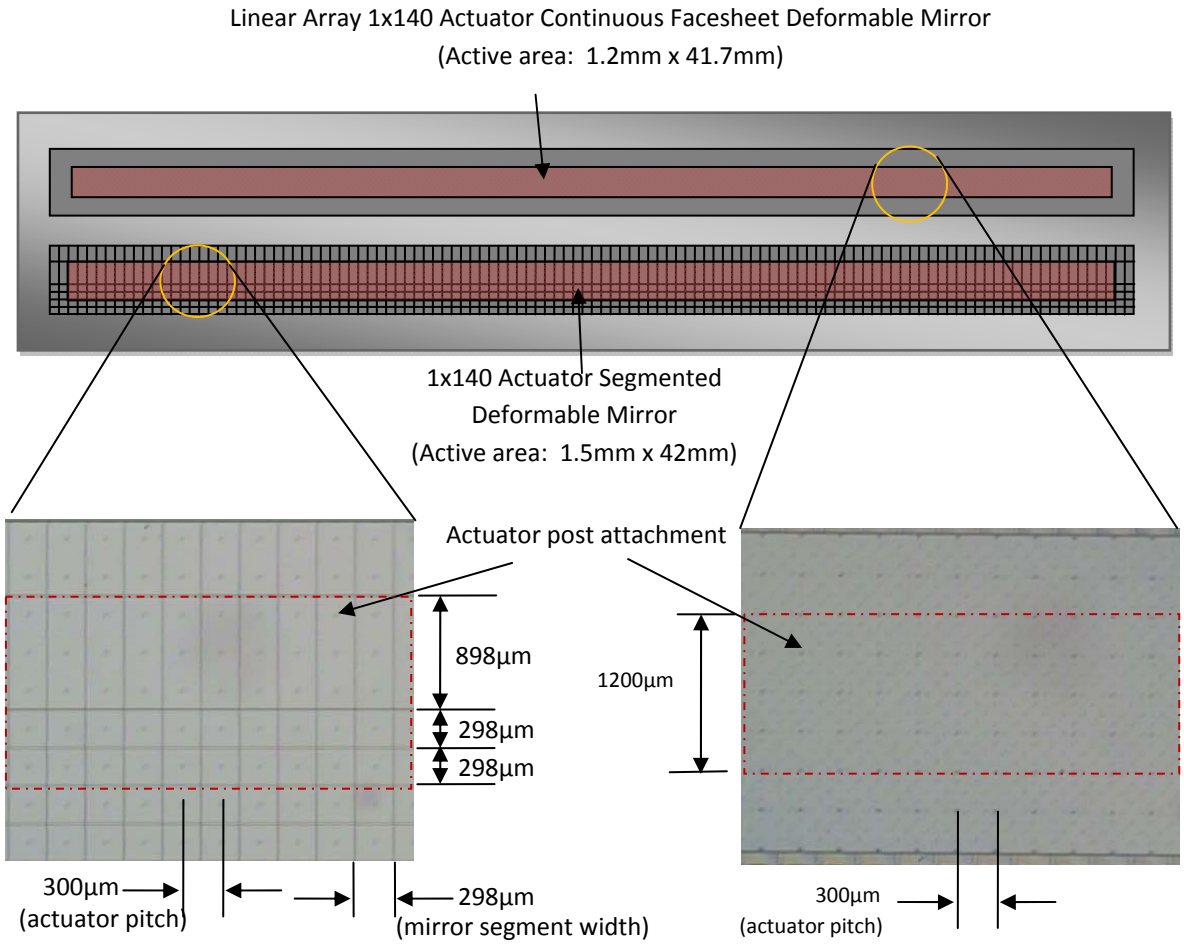

Figure 6. Overview of 1x140 DM layout with images of a 1x10 sub-array of the segmented (Left) and continuous (Right) facesheet DMs. Each active row of the DM consists of five actuators ganged together to act in concert. The segmented DM is divided into three separate segments of one 898µm and two 298µm wide segments

The segmented DM has mirror segments that are nominally 298µm wide leaving gaps of 2µm between segments. The array has been designed with two 298µm and one 898µm long segments to allow the user to experiment with different beam widths of up to ~1.5mm wide. Due to the influence of neighboring actuators the effective maximum width of the incident beam onto the continuous facesheet device is 600µm. A surface profile of a 1x140 continuous facesheet DM with a single row actuated is shown in Figure 7. It can be seen from this profile that the edges of this

region do not have the same deflection as the center 600µm region which is due to the upward restoring force induced by the dummy actuators on the edges of the array.

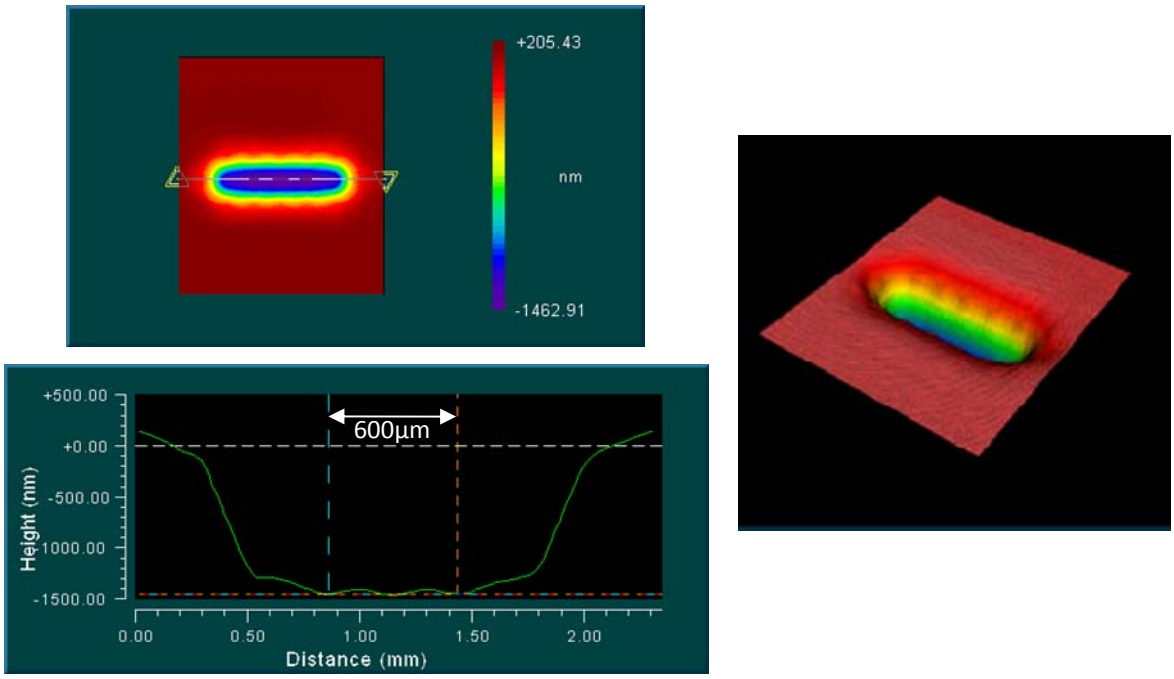

Figure 7. Profile of the surface figure of a Liner Array 1x140 continuous facesheet DM with a single row actuated to ~1500nm. Due to the influence of the inactive edge actuators only the center 600µm of the active row achieves the full deflection.

Unpowered Surface Figure

The DM is manufactured using polysilicon surface micromachining processes which include a number of polishing steps to yield a high-quality mirror surface with a small scale roughness of less than 2nm RMS. Due to the conformal nature of surface-micromachining, some periodic features resulting from the mirror attachment posts, and underlying structures (print-through), as well as etch access holes, remain on the mirror surface resulting in a single actuator sub-aperture surface roughness of ~6nm RMS (see Figure 8). The local surface figure of the continuous and segmented facesheet DM are shown in Figures 8 and 9, respectively, on which the structured (high-frequency) surface features resulting from print-through can be seen. Each single actuator sub-aperture of the continuous facesheet DM is measured to have a surface figure of ~6nm RMS. Each sub-aperture has eight small (6µm x 6µm) holes in the mirror facesheet, required for device manufacturing, yielding a fill factor of 99.6%. The 298µm x 298µm and 898µm x 898µm mirror segments of the segmented facesheet DM have a surface figure of 13nm RMS and 30nm RMS, respectively.

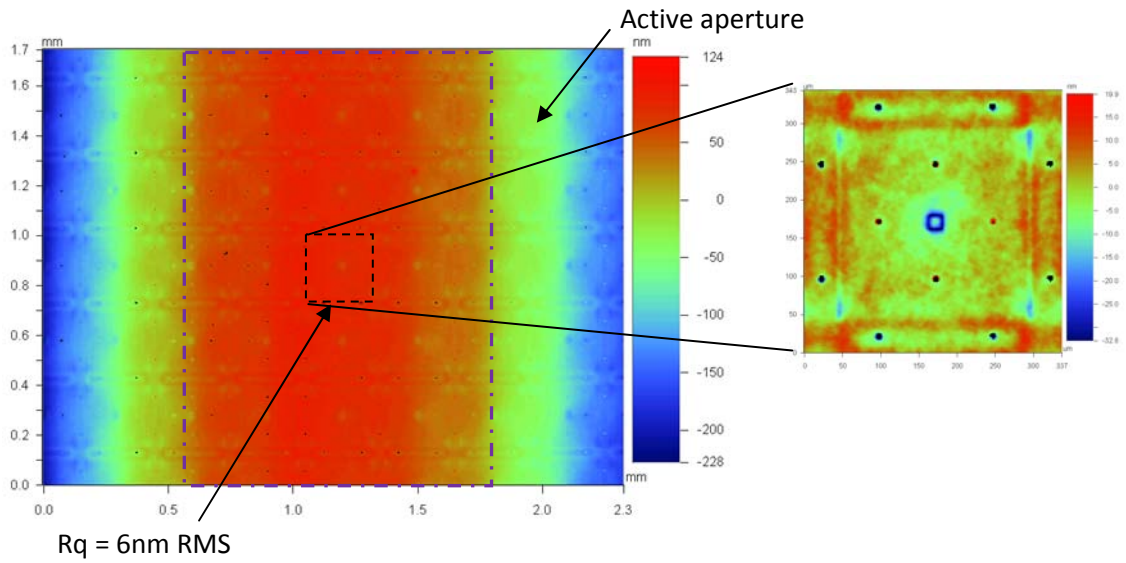

Figure 8. Local surface figure measurement of a continuous facesheet Linear Array DM. Each 300µm x 300µm single actuator sub-aperture has a surface figure of 6nm RMS. The surface details of a single actuator sub-aperture (with low-order terms removed) shows the period surface features resulting from the surface-micromachining manufacturing process.

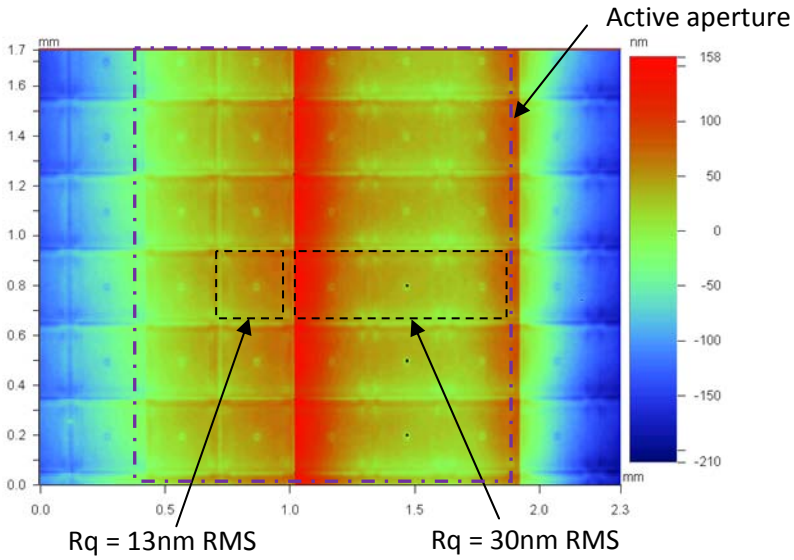

Figure 9. Local surface figure measurement of segmented facesheet Linear Array DM. Each 298µm x 298µm and 898µm x 898µm mirror segment has a surface figure of 13nm RMS and 30nm RMS respectively.

The unpowered surface figure of the Linear Array DM is shown in Figure 10. As shown in this Figure, the device exhibits a low order figure error consisting mainly of curvature with a ROC of ~48m and peak-to-valley deviation from flat of 4.6µm. This unpowered surface figure error cannot be corrected with the DM actuators alone since the stroke of the device is limited to ~2µm. Typically, this low-order error is corrected in the optical system by positioning a lens in the imaging system to compensate for the DM curvature.

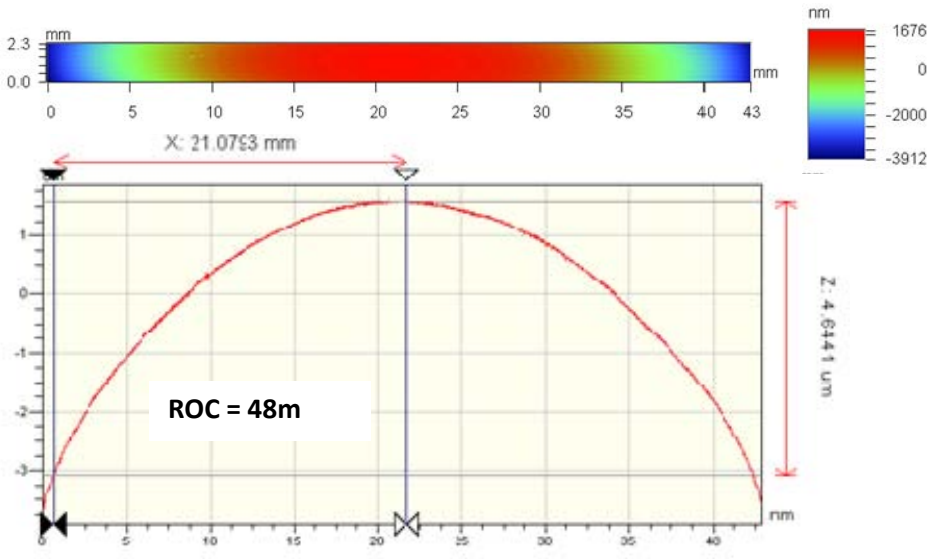

Figure 10. Surface measurement of the unpowered Linear Array DM. The device has a radius of curvature of 48m resulting from bow of the substrate, with ~4.6µm peak-to-valley error over the active aperture.

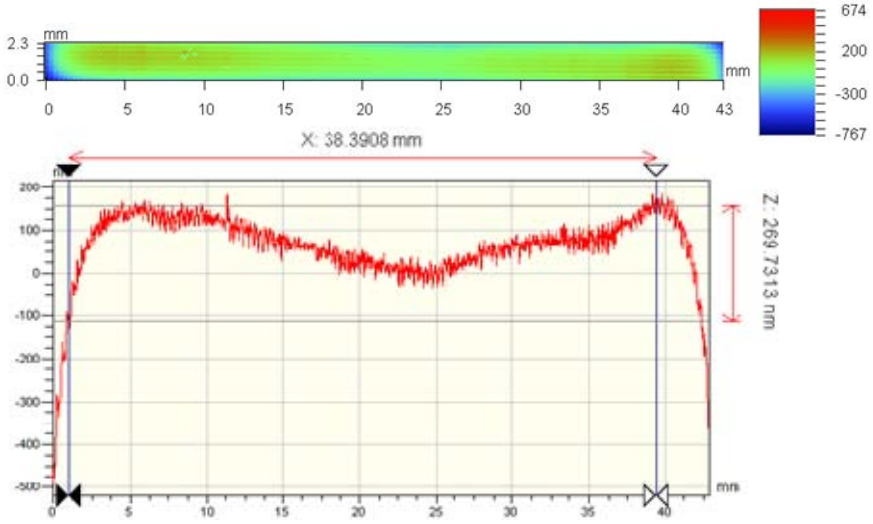

Figure 11. Residual surface figure error of the unpowered Linear Array DM with low-order spherical term removed. The peak-to-valley surface figure error that remains is 270nm.

Electro-Mechanical Performance

A characteristic curve of actuator deflection as a function of applied voltage is shown in Figure 12. The maximum achievable deflection of the DM is measured by applying a voltage to 4 rows of actuators to eliminate the effects of the influence function. A mechanical stroke of over 2µm can be achieved by applying 220V to the actuators. Since electrostatic actuation is used to deflect the mirror surface, the actuators exhibit no hysteresis and therefore have very good go-to repeatability making the device well suited for open-loop control or switching between predefined mirror shapes with minimal error.

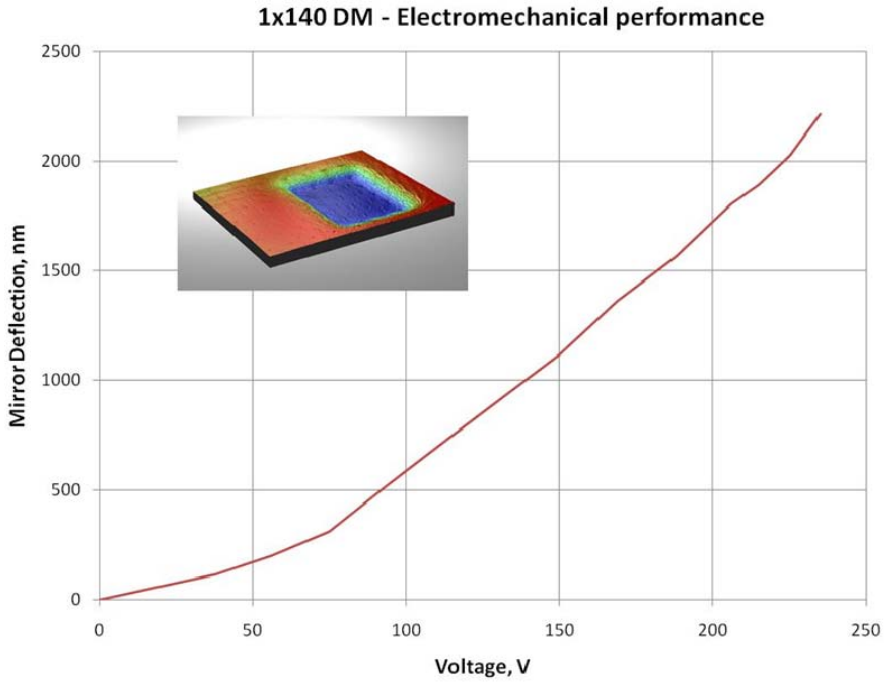

Figure 12. Typical mirror deflection as a function of applied voltage measured on a 4 row wide sub-aperture of the DM to eliminate the effects of the influence function. At 220V a deflection of 2µm, corresponding to 4µm optical path difference (wavefront), is achieved.

Linear Array DM System

The Linear Array DM is controlled using the 140 channel BMC Multi-Driver electronics with 14-bit resolution. The driver connects to the DM board using four (4) 37-pin D-Sub connectors and can be controlled using a PC through a USB interface. The DM assembly and drive electronics unit are shown in Figure 13.

Figure 13. Linear Array DM Prototype system with 14-bit Multi-Driver electronics.

Application Overview

Fast and Precise Laser Pulse Compression

Credit: Reto Fiolka, Janelia Farm Howard Hughes Medical Institute (HHMI)

The Linear Array has proven to enable fast and precise laser pulse compression when tested by researchers at HHMI's Janelia Farm Research Campus. Ultrafast lasers are useful in many applications within spectroscopy, photochemistry, laser processing and microscopy. However, to make the most use of such short laser pulses, a pulse compressor is needed to compensate for the dispersion induced by optical elements. Liquid crystal-based spatial light modulators (SLM)[1] are most commonly used in laser pulse compressors. Although a proven technology in display applications, liquid crystals have drawbacks including phase jitter and a limited fill factor. To address these obstacles Janelia Farm's Reto Fiolka turned to BMC's prototype Linear Array Deformable Mirror (DM).

Methods and Setup

The setup used at Janelia Farm is schematically shown in Figure 14. Laser light, centered around 790 nm and with 100 nm spectral width, is diffracted by a blazed grating (600 grooves/mm, Model: 10RG600-800-1, Newport, Irvine, CA). The first diffraction order is incident on a concave mirror which focuses the individual wavelength components on the Linear Array DM. For clarity, only the center wavelength (790 nm) is shown in Figure 14. The Linear Array DM is slightly inclined such that the light is back-reflected slightly upwards. The laser pulse is recombined by the grating and about one meter away from the compressor the reflected laser beam is picked up with a small mirror. For their experiments the segmented section of the Linear Array DM was used, since the optimization algorithm requires independent actuation of pixels. The pixel stroke was calibrated at different locations on the segmented DM and the measurement was repeated each month. The values are in good agreement with each other and thus the phase calibration remained valid over extended periods of time.

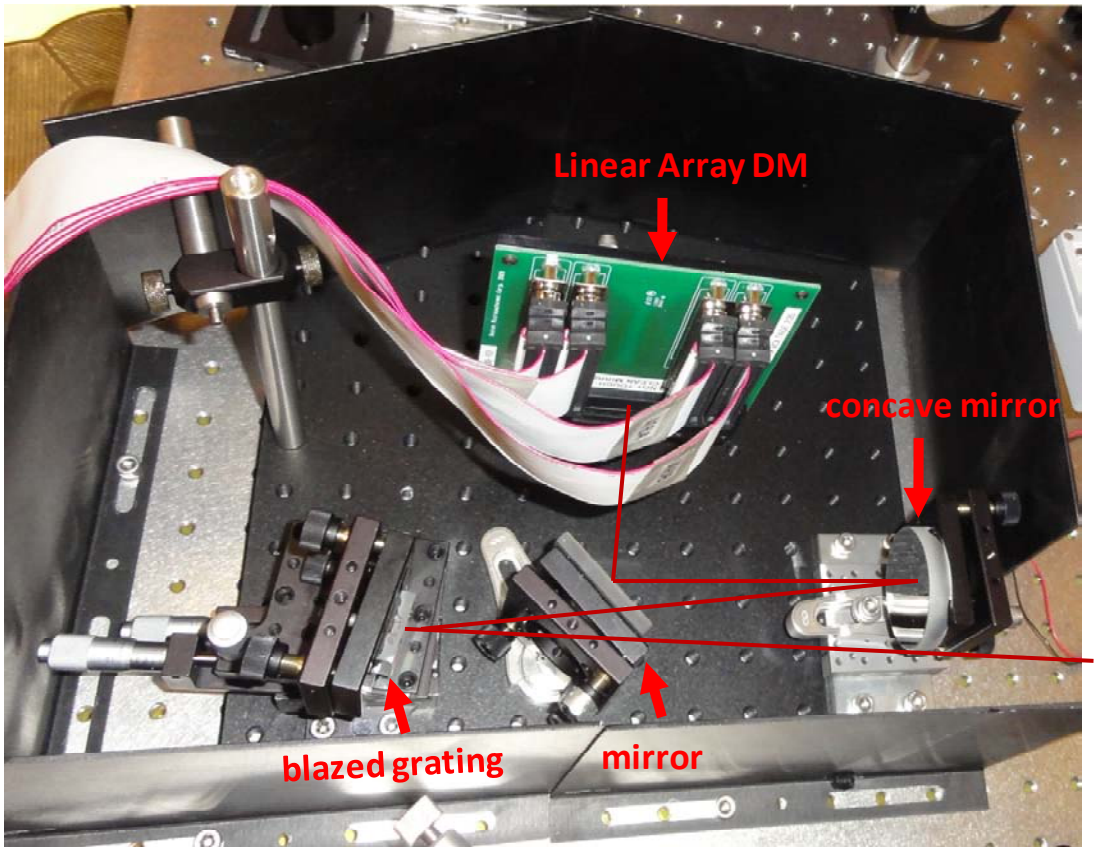

Figure 14. Experimental setup for pulse compression using the Boston Micromachines Linear Array DM.

The spectral phase was optimized by phase resolved interferometric spectral modulation (PRISM)[2]. In PRISM, a group of segments of the DM are phase modulated at different drive frequencies and the variation of a nonlinear signal (e.g. two photon fluorescence) is measured. This signal is Fourier transformed in time and the phase at the individual drive frequencies is recovered and displayed on the corresponding pixels. Using this technique, the optimal spectral phase to maximize the nonlinear signal (corresponding to the shortest pulse duration) is determined. One round of PRISM was completed in less than 0.7s and the correction speed was mainly limited by Janelia Farm's control software.

Evaluation

To evaluate the performance of the pulse compressor, the laser pulses were analyzed with frequency resolved optical gating (FROG)[3] using a commercial instrument (Grenouille, Swamp Optics, Atlanta, GA). In Figure 15a and b, the temporal and spectral profile of the pulse is shown when a flat wavefront is displayed on the DM. Evidently, the pulse is distorted and the spectral phase is not flat at all (a flat spectral phase is required for a transform limited pulse). Next, the beam returning from the pulse compressor was focused with a concave mirror onto a GaAsP photodiode and the resulting nonlinear signal was used as a feedback for the PRISM algorithm. After the PRISM optimization, the temporal profile (Figure 15c) shows a dramatically shorter, Gaussian shaped pulse. The spectral phase is perfectly flat (Figure 15d) with less than 0.01 radians

phase error and is stable in time. These results suggest that the precision and stability of the Linear Array DM allows close to perfect restoration of transform limited laser pulses.

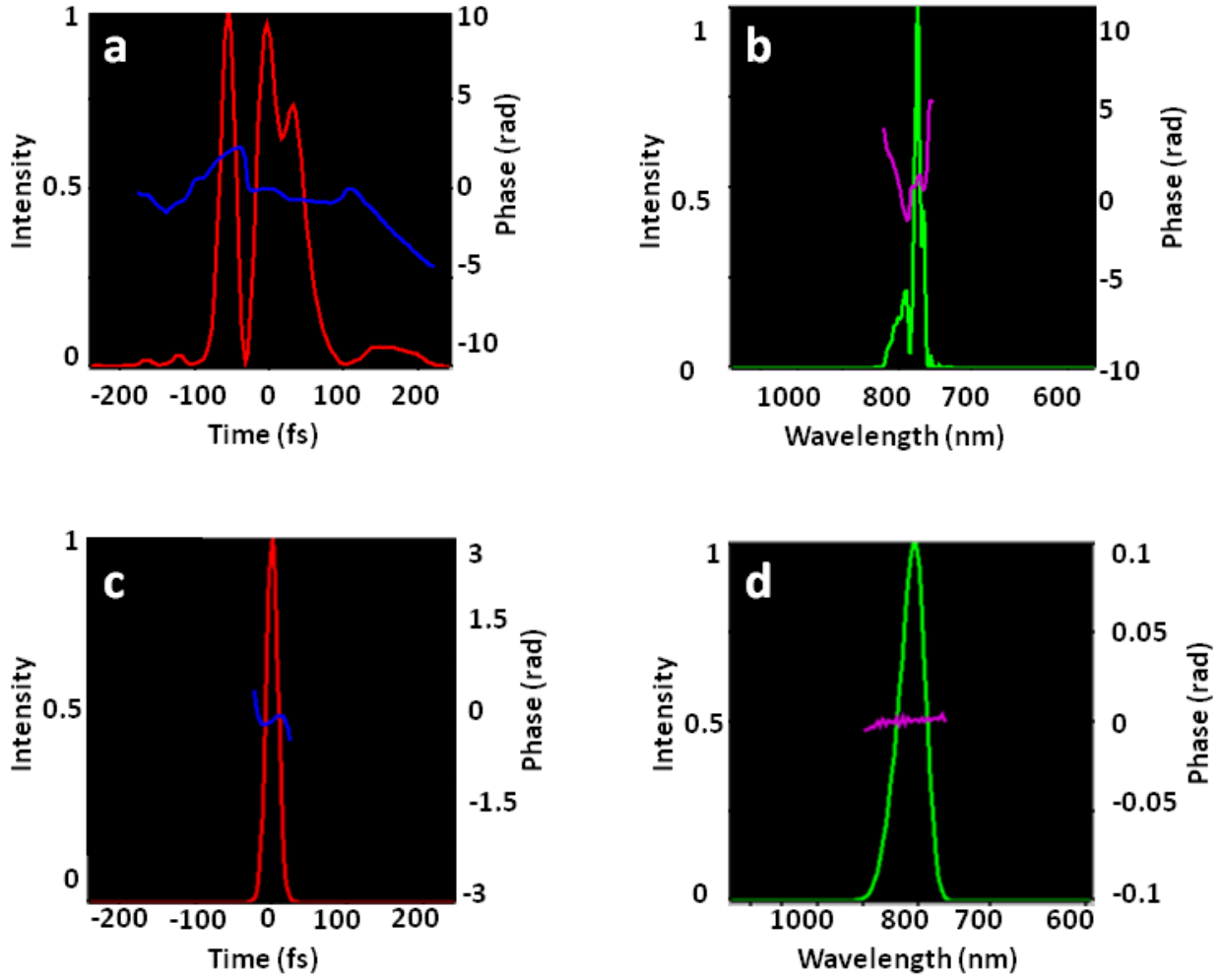

Figure 15. Frequency resolved optical gating (FROG) measurements. ***a*** *Temporal intensity (red) and phase (blue) of the uncorrected laser pulse.* ***b*** *Spectral intensity (green) and phase (purple) of the uncorrected laser pulse.* ***c*** *Temporal intensity (red) and phase (blue) of the optimized laser pulse. The pulse width totals 19.8 fs.* ***d*** *Spectral intensity (green) and phase (purple) of the optimized laser pulse.*

Application Demonstration

Pulse Compression for Two Photon Microscopy

Credit: Reto Fiolka, Janelia Farm HHMI

To illustrate the use of the Linear Array's potential as a pulse compressor for imaging applications, Janelia Farm performed two photon fluorescence microscopy. The Linear Array pulse compressor setup was used to restore the laser pulse to its transform limited state, thus improving the ability to excite fluorescence by two photon absorption. A sample consisting of 10 micron diameter fluorescence beads (emission: 465 nm) was prepared and spread on a cover-slip. The laser beam first propagated through the pulse compressor and was subsequently focused on the sample using a 20X NA 0.5 Nikon objective. A 2D image was obtained by translating a motorized sample stage. Without spectral pulse shaping, only a weak fluorescence signal could be obtained (Figure 16a & c). Since the objective adds significant additional dispersion to the laser pulse, the spectral phase correction that had been determined previously using the photodiode could not be used. Therefore PRISM optimization was repeated using the fluorescence signal coming from the beads itself as a feedback signal.

Janelia Farm's results show a dramatic increase in fluorescence signal for the optimized spectral phase (Figure 16b & d). The signal strength was increased by a factor of ~6.5.

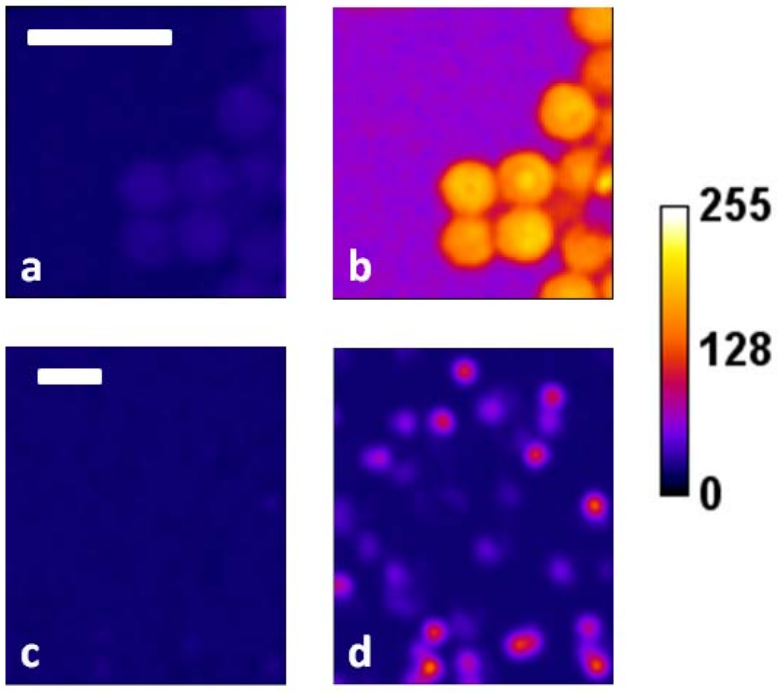

*Figure 16. Two photon microscopy of 10 micron diameter fluorescent beads. **(a)** & **(c)** Fluorescence image obtained with a flat wavefront on the DM. **(b)** & **(d)** Fluorescence image after the spectral phase was optimized with 5 PRISM iterations. Scale bar: 25microns. Color bar in arbitrary intensity units, all images have the same scale.*

Fiolka concluded, “The tested device represents a promising alternative to liquid crystal displays, since the MEMS technology enables high fill factor, high efficiency and operation speed, exceptional phase stability and accuracy and can be used over a very broad wavelength spectrum.”

References:

1. Lozovoy, V.V., Pastirk, I. & Dantus, M. Multiphoton intrapulse interference.IV. Ultrashort laserpulse spectral phase characterization and compensation. *Opt. Lett.* 29, 775-777 (2004).
2. Wu, T.-w., Tang, J., Hajj, B. & Cui, M. Phase resolved interferometric spectral modulation (PRISM) for ultrafast pulse measurement and compression. *Opt. Express* 19, 12961-12968 (2011).
3. Trebino, R. & Kane, D.J. Using phase retrieval to measure the intensity and phase of ultrashort pulses: frequency-resolved optical gating. *J. Opt. Soc. Am. A* 10, 1101-1111 (1993).

For additional information on device performance and availability please contact:

Boston Micromachines Corporation
30 Spinelli Place
Cambridge, MA 02138
617-868-4178
info@bostonmicromachines.com